International Journal of Engineering and Science Invention (IJESI)
ISSN (Online): 2319-6734, ISSN (Print): 2319-6726
www.ijesi.org ||Volume 15 Issue 2 February 2026 || PP 44-50

A Study on Nonlinear Electrostatic Wave Structures in Lunar Plasma Environments

Sumit Singh[1], Dr. Pradeep Kumar Dubey[2]
[1, 2] *Department of Physics, Mansarovar Global University, Sehore, MP*

ABSTRACT
Another mechanism of the generation of the electrostatic waves observed in the lunar wake during the first flyby of the ARTEMIS mission is proposed, which relies on slow and fast ion-acoustic solitons and electron-acoustic solitons. The lunar wake plasma is a multicomponent magnetized plasma fluid containing hot protons, hot heavier ion, 2-He ions (He++), electrons beam, and suprathermal electrons which obey the kappa distribution. The plasma model contains heavy ions, electron beams, and hot protons, and suprathermal electrons which are in a kappa distribution. We build up and explore the conditions of existence and propagation of electrostatic solitary waves by Sagdeev pseudopotential formulation. The results indicated the formation of various prohibited propagation and coexistence regimes and positive and negative potential solitons. It is found that vital plasma factors are of significant influence to the properties of slow and rapid ion-acoustic modes brought about by the electron beam velocity and ion temperature ratios. Also, in the plasma density conditions, the electron-acoustic modes are shown to support just the negative polarity solitons.
KEYWORDS: *Electrostatic, Solitary waves, Suprathermal, Lunar wake, Electrons*

I. INTRODUCTION

Earth, Mars, Venus, the Moon, Saturn, and many more planets' magnetospheres are replete with electrostatic solitary waves (ESWs). Depending on the strength of the magnetic field, they can be seen as electric field structures that are bipolar, monopolar, or tripolar. Broadband electrostatic noise with frequencies ranging from the ion cyclotron frequency to the local electron plasma frequency is what ESWs represent in the frequency domain. It is common for these formations to be associated with ion/electron beams or field-aligned streaming instabilities such the two-stream, bump-on-tail, or Buneman instability. Theoretical investigations into the mechanism of ESW creation on several planets and the Moon have recently surged in response to the importance of ESWs in particle acceleration and the maintenance of parallel acceleration in the space plasma environment.

The production of ESWs in the solar wind-permeated Venusian ionosphere by means of a five-component plasma that includes Venusian H+ and O+, background electrons, and electrons and protons from the solar wind. The features of ESWs are considerably impacted by the fluctuation in the ratio of ions' temperatures and the density of solar wind proton beams. Martian electronegative plasma, which contains positive and negative ions as well as two separate populations of κ-distributed electrons, and the presence and behavior of ESWs. the possibility that Mars hosts solitons and supersolitons of both positive and negative polarity. the magnetosheath on Mars has a double-layer (DL) structure. According to the three-species plasma model with positive ions and warm and colder electrons, the observed DLs can be described as electron-acoustic DLs. In an electric field, DLs—which are confined plasma structures—appear as structures with one pole. Both the acceleration of particles and the loss of energy rely on them. how ESWs in Saturn's magnetosphere have developed through time using a fluid with both hot and cold electrons as well as stationary ions. The κ-distribution was thought to be followed by the heated electrons. The solitary waves in Saturn's magnetosphere that are caused by dust.

Electrostatic waves (ESWs) are generated in the lunar wake by a plasma that is composed of protons, α particles, electrons, and suprathermal electrons. This plasma is responsible for the creation inside the lunar wake. When it comes to electron-acoustic solitons and ion-acoustic solitons, both slow and rapid, the discoveries that pertain to these kinds of forces are discussed. DIAWs, which are also known as dielectric-induced acoustic waves, originate from the dust plasma that is found in Saturn's F ring layer. In the event that the system is functioning in the nonlinear region, the shear-modified DIAW is utilized to generate electrostatic solitons! Within the dusty plasma environment of the Jovian magnetosphere, an examination was carried out to determine whether or not dust-acoustic solitons are present. It is possible that the positive dust charge, which is present in both the solitary waves and the magnetosphere as a whole, has a role in deciding whether or not solitary particles coexist in the magnetosphere of a Jupiter that is magnetically unclean. The features of the waves are influenced by the surrounding magnetic field, which in turn has an impact on the breadth and amplitude of dust ion-acoustic solitary waves that are traveling through Jupiter's magnetosphere.

Juno performed an unprecedented flyby of Ganymede on June 7, 2021, at an altitude of around 1046 km. As Juno drew near Ganymede, it did so from the night side, through its magnetosphere, the heretofore uncharted wake zone, the dayside, and eventually Jupiter's plasma disk. Juno detected whistler-chorus and hissing in the magnetosphere as well as electron cyclotron harmonic emissions with a band at the higher hybrid frequency during the flyby. The wake area and the magnetopause boundary both showed evidence of ESWs and low-frequency turbulence. The latter source examined a five-part model that included heated H+ and O+ ions, a two-counter-flowing electron beam, and suprathermal electrons that followed the κ-distribution. This flyby is a once in a lifetime chance to bring theory in line with observations by revealing intricate details about the plasma wave characteristics and the background plasma environment.

The biggest moon in our solar system, Ganymede also happens to be the only one with its own intrinsic magnetic field, which is a unique quality. Consequently, within Jupiter's large-scale magnetosphere, a mini-Ganymede magnetosphere continues to exist. Plasma waves, electric currents along the magnetopause, and Alfvén wings are produced when the Ganymede magnetosphere interacts with the Jovian plasma at a sub-Alfvénic velocity. Bow shock does not develop upstream because the flow is subsonic. On Ganymede, the magnetosphere is closed at the equator and open at the polar cap; the former has both footpoints on the Moon and the latter on Jupiter's ionosphere. Both Ganymede and Jupiter experience magnetic reconnection at their upstream magnetopauses because their dipole fields are almost perpendicular to one another. The dynamics of Ganymede's magnetosphere are thought to be driven in large part by the magnetic reconnection.

With data from the Jovian Auroral Distributions Experiment (JADE), the plasma characteristics were examined during the Juno wake pass. Juno was likely moving over the open field lines that link Ganymede to Jupiter since its plasma composition was determined to be essentially identical to Jupiter's plasma disk: H+, H2+, O+, S2+, O2+, S3+, S+, and O3+. On the other hand, they first documented the presence of H3+ and H2+ ions in the wake region and in the vicinity of Ganymede, which suggests that molecules and ions coming from surface or atmospheric water are influencing the area surrounding Ganymede. Approximately (0.1-2) KeV was found to be the energy of the light ions, whereas approximately (1-20) KeV was the energy of the heavy ions. Within the wake, the intensity of the low-energy field-aligned electrons, which range from around 0.1 to 1 KeV, was found to be increased by a factor of up to about 3.5. The density of heavy ions (5.7-24 cm^{-3}) and hydrogen ions (H+ ions) ranges from around 0.7-2.3 cm^{-3}, respectively.

II. REVIEW OF LITERATURE

Rasca, Anthony et al., (2022) Downstream of the lunar surface at night, a low-density wake area develops in the solar wind. The reaction of the lunar wake to a passing coronal mass ejection (CME) is modeled in this work using a series of 3D hybrid particle-in-cell simulations. The average plasma properties were calculated on June 22, 2015, from data collected by the Wind satellite at 1 au during three separate stages of a passing halo (Earth-directed) CME. As the time-static upstream boundary conditions for three independent simulations, we employ each set of plasma parameters—representing the shock/plasma sheath, a magnetic cloud, and plasma circumstances we term the mid-CME phase. The outcomes of these models are subsequently contrasted with models that employ standard solar wind parameters. During the plasma sheath phase of the CME, the results reveal a plasma void that is shorter than nominal circumstances and a distinct rarefaction cone that starts at the terminator. In contrast, a plasma void that is much longer is formed during the magnetic cloud and mid-CME phases. In the plasma sheath phase, electric and magnetic field intensifications are seen along the central wake, and in the magnetic cloud and mid-CME phases, electrostatic turbulence is dominant along the plasma void boundaries and 2-3 lunar radii R M downstream from the center wake. As the upstream solar wind changes during a CME, the models show that the lunar wake reacts dynamically.

Chu, Feng et al., (2021) Several intriguing phenomena, including electrostatic instabilities and waves, can occur when a substantial percentage of the electrons and ions from the solar wind are dispersed above lunar crustal magnetic anomalies and then redirected into the flow of the solar wind. Interactions between these electrostatic structures and the plasma in the background can potentially cause heating and scattering of electrons. Our investigation involves examining data collected from the ARTEMIS satellite in order to learn about the electron heating and electrostatic waves that have been measured over the lunar magnetic anomalies. According to our findings from examining two lunar flybys in 2011 and 2013, the electron cyclotron drift instability (ECDI) and electron two-stream instability (ETSI) might be significant factors propelling the electrostatic waves. Additionally, we discover that ECDI and the modified two-stream instability (MTSI) might be the processes that cause significant isotropic electron heating across the lunar magnetic anomalies.

Lakhina, Gurbax et al., (2021) Space plasmas, such as the solar wind, the lunar wake, and the magnetospheres of the planets, are rife with electrostatic solitary waves (ESWs). The observable features of the ESWs have been explained by a number of theoretical hypotheses. The models may be grouped into two basic types: ion- and electron-acoustic solitons and Bernstein-Green-Kruskal (BGK) modes/phase space holes. Within the space community, models based on BGK modes/phase space holes have been increasingly favored. The

possibility of using soliton models to describe ESW properties has just now come to light. The purpose of this paper is to summarize the state of the art on the ion- and electron-acoustic solitons as well as the double layers model in space plasmas with many components. All plasma species are treated as fluids in these models with the exception of the energetic electron component, which is controlled by either a kappa distribution or a Maxwellian distribution. In addition, the models take into account the nonlinear electrostatic waves that are moving in a parallelogram with the surrounding magnetic field. The relevance of the link between ESW space measurements and theoretical models is emphasized. Through a comparison of theoretical predictions and observations of ESWs in space plasmas, several particular applications of ion- and electron-acoustic solitons/double layers will be explored. The ESWs seen in space plasmas can be explained by the ion- and electron-acoustic solitons/double layers concepts.

Morozova, T.et al., (2015) The article details a plasma-dust system located in the near-surface layer of the sunlit Moon. Photoelectrons, neutrals, charged dust grains, and electrons and ions from the solar wind are all part of the system. Waves in the plasma close to the Moon's surface, both linear and nonlinear, are addressed. It is observed that the velocity distribution of photoelectrons can be described as a superposition of two distribution functions with different electron temperatures: photons with energies close to the regolith's work function knock out lower energy electrons from the lunar regolith, and photons with energies corresponding to the peak at 10.2 eV in the solar radiation spectrum knock out higher energy electrons. The solar wind's motion with regard to photoelectrons and dust grains distorts the anisotropy of the electron velocity distribution function, causing instability and exciting high-frequency oscillations in the Langmuir and electromagnetic wave ranges. It is also possible to stimulate dust acoustic waves, as seen, for instance, close to the lunar terminator. The parameters of the dust-plasma system at the near-surface layer of the lighted Moon's surface are discovered to have solutions in the form of dust acoustic solitons. The soliton amplitude and Mach number ranges are found.

Haakonsen, Christian et al., (2015) A 1D electrostatic particle-in-cell (PIC) model of the solar wind wake behind the moon is used to study it, in contrast to previous studies, using a physical ion to electron mass ratio. The model is further generalized to describe the supersonic passage of dense magnetized plasma past non-magnetic objects. An investigation into the ion stability without kinetic electron effects is initiated by using a hybrid electrostatic Boltzmann electron treatment. The results demonstrate that, at downstream wake distances (in lunar radii) exceeding about three times the solar wind Mach number, the ions are two-stream unstable. Next, we employ PIC electron simulations to demonstrate that kinetic electron effects can cause ion beam disruption at least three times closer to the moon than in the hybrid counterparts. The non-linear expansion of electron holes produced by a tiny depression in the electron velocity distribution is a new wake phenomena that causes this disturbance. While the majority of the dimple-induced holes are tiny and swiftly exit the wake, roughly tracking the unaltered electron phase-space paths, a small number of holes, located closer to the wake's center, persist and eventually enlarge to the point where they interrupt the ion beams. To fully grasp the 1D electrostatic stability of these wakes, non-linear kinetic-electron effects are crucial; potential observable signals in the lunar wake data from ARTEMIS are thus examined.

Hashimoto, Kenichiro et al., (2010) We report on Selene's (Kaguya) observations of electrostatic solitary waves (ESWs) in the solar wind and the lunar wake near the Moon. SELENE, a 100 km lunar orbiter, has recorded a variety of electromagnetic fields, including wave electric fields, background magnetic fields, ion and electron fluxes, and more. Type A ESWs are produced by electrons accelerated and reflected by an electric field in the wake boundary; Type B ESWs are produced by bi-streaming electrons mirror-reflected over the magnetic anomaly; and Type C ESWs are produced by reflected electrons when the local magnetic field is coupled to the lunar surface. The three types of ESWs are classified according to the regions of observation. Langmuir waves frequently alternate with ESWs of Type C.

III. THEORETICAL MODEL

The plasma that forms in the lunar wake is a four-component model that is homogenous, collisionless, magnetized, and made up of hot protons, hot heavier ions (He++), an electron beam, and suprathermal electrons that follow the κ-distribution, as described by:

$$f_e(v) = \frac{N_{e0}}{\sqrt{\pi}\theta} \frac{\Gamma(\kappa+1)}{\kappa^{3/2}\,\Gamma(\kappa-1/2)} \left(1+\frac{v^2}{\kappa\theta^2}\right)^{-(\kappa+1)} \tag{1}$$

In this context, Γ(κ) is the gamma function, κ is the spectral index where κ > 3/2, and θ is the modified electron thermal speed, which is determined by

$$\theta^2 = \left(2-\frac{3}{\kappa}\right)\frac{T_e}{m_e}$$

At this point, the electron equilibrium number density is denoted by Ne0. The temperature of an electron is Te, while its mass is me. It is believed that the ESWs are moving in a parallel fashion to the Earth's magnetic field. The normalized multifluid equations that control the system are:

Continuity equation

$$\frac{\partial n_j}{\partial t}+\frac{\partial (n_j v_j)}{\partial x}=0 \tag{2}$$

Momentum equation

$$\frac{\partial v_j}{\partial t}+v_j\frac{\partial v_j}{\partial x}+Z_j\mu_{pj}\frac{\partial \phi}{\partial x}+3\mu_{pj}\sigma_j\frac{n_j}{n_{j0}^2}\frac{\partial n_j}{\partial x}=0 \tag{3}$$

Poisson's equation

$$\frac{\partial^2\phi}{\partial x^2}=(n_e+n_b-n_p-Z_i n_i) \tag{4}$$

The velocities are normalized with the ion-acoustic speed in equations (2)-(4), and the number densities are normalized by the overall equilibrium number density, N0 = Np0+ZiNi0 = Ne0+ Nb0, $C_a=\sqrt{T_e/m_p}$, lengths with the effective hot electron Debye length, $\lambda_{de}=\sqrt{T_e/4\pi N_0 e^2}$, time with the inverse of the effective proton plasma frequency, $f_{pp}=\sqrt{4\pi N_0 e^2/m_p}$ and electrostatic potential, φ by Te/e.

The mass of the proton (mp) and the mass of the jth species (mj) are used in this context, where μp j = mp/mj. The normalized equilibrium number density of the jth species is calculated as σj = Tj/Te and nj0 = Nj0/N0. "e" stands for the electrical charge. A fluid's normalized velocity is denoted by vj. For proton, Zj is equal to 1, for heavier ion (alpha particle), Zj is equal to 2, and for beam electron, Zj is negative 1.

The adiabatic index γj = 3 has been taken into account for every species. For this particular one-dimensional instance, this is appropriate. A stationary frame is used to turn the previous set of equations into the phase velocity of an electrostatic solitary wave, denoted as ξ = x − Mt, where M = V/Ca is the Mach number. The formula for the Sagdeev pseudopotential is obtained by solving these equations with the proper boundary conditions.

$$\begin{aligned}S(\phi,M) \;=\; & \frac{n_{p0}}{6\sqrt{3\sigma_p}}\left[\left(M+\sqrt{3\sigma_p}\right)^3-\left\{\left(M+\sqrt{3\sigma_P}\right)^2-2\phi\right\}^{3/2}-\left(M-\sqrt{3\sigma_p}\right)^3+\left\{\left(M-\sqrt{3\sigma_p}\right)^2-2\phi\right\}^{3/2}\right]\\ & +\frac{n_{i0}}{6\sqrt{3\sigma_i}}\left\{\left(\frac{M}{\sqrt{\mu_{pi}}}+\sqrt{3\sigma_i}\right)^3-\left[\left(\frac{M}{\sqrt{\mu_{pi}}}+\sqrt{3\sigma_i}\right)^2-2Z_i\phi\right]^{3/2}-\left(\frac{M}{\sqrt{\mu_{pi}}}-\sqrt{3\sigma_i}\right)^3+\right.\\ & \left.\left[\left(\frac{M}{\sqrt{\mu_{pi}}}-\sqrt{3\sigma_i}\right)^2-2Z_i\phi\right]^{3/2}\right\}+\frac{n_{b0}}{6\sqrt{3\sigma_b}}\left\{\left(\frac{M-V_{b0}}{\sqrt{\mu_{pe}}}+\sqrt{3\sigma_b}\right)^3-\left[\left(\frac{M-V_{b0}}{\sqrt{\mu_{pe}}}+\sqrt{3\sigma_b}\right)^2+2\phi\right]^{3/2}\right.\\ & \left.+\left[\left(\frac{M-V_{b0}}{\sqrt{\mu_{pe}}}-\sqrt{3\sigma_b}\right)^2+2\phi\right]^{3/2}-\left(\frac{M-V_{b0}}{\sqrt{\mu_{pe}}}-\sqrt{3\sigma_b}\right)^3\right\}+n_{e0}\left[1-\left(1-\frac{\phi}{\kappa-3/2}\right)^{-\kappa+3/2}\right]\end{aligned} \tag{5}$$

IV. RESULTS AND DISCUSSIONS

The slow ion-acoustic soliton's existence curve is shown against Vb0 in Figure 1, with the following normalized parameters: ni0 = 0.05, nb0 = 0.02, σp = 0.3, σi = 0.5, σb = 0.002, and κ = 6. Positive potential solitons are seen in region-I, where 0≤ Vb0<4, and negative potential solitons in region-II, where 4≤ Vb0<5.4. The banned gap corresponds to Region III, defined as 5.4≤ Vb0< 6.1. A forbidden gap is an area where solitons are unable to spread. Then, between the two red-dashed lines, there is an area where both polarity solitons coexist (regionIV, 6.1≤ Vb0 ≤ 7).

Here we can see that there are negative potential solitons represented by the pink circles and positive potential solitons by the green + signs. Solitons with positive potentials (Region-V) exist when Vb0 > 7. Requiring that the number density of ions, ni, remain real limits the greatest feasible amplitude of the slow ion-acoustic positive polarity soliton, whereas the number density of beam electrons, nb, limits the maximum possible amplitude of the negative polarity solitons.

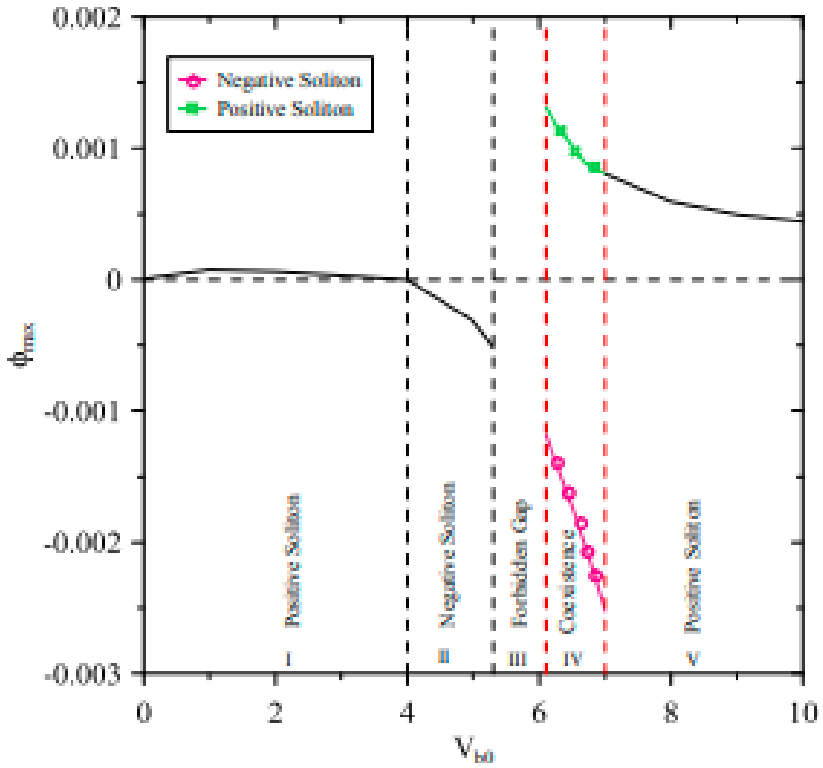

Figure 1: Variation of existence regions of slow ion acoustic solitons with respect to beam velocity Vb0

The rapid ion-acoustic soliton's existence curve with respect to Vb0 is displayed in Figure 2, with the normalized parameters ni0 = 0.05, nb0 = 0.02, σp = 0.3, σi = 0.5, σb = 0.002, and κ = 6. Positive potential solitons are seen in region-I, where 0≤ Vb0< 5, while negative potential solitons are seen in region-II, where 5≤ Vb0< 6.1. After that, in region-III, there is an excluded interval where Vb0 is between 6.1 and 11. Region-IV, where 11 ≤ Vb0< 12, represents the solitons with negative potential. Coexistence of both polarity solitons is shown by the region between the two red-dashed lines (Region-V, 12≤ Vb0 ≤ 19). Positive potential solitons are shown by the blue + signs, whereas negative potential solitons are depicted by the pink circles.

Positive potential solitons (Region-VI) are present when Vb0 > 19. As long as the proton density, np, remains genuine, the maximal amplitude of the positive polarity fast ion-acoustic soliton can be achieved. A rapid ion-acoustic soliton with a negative potential has an amplitude restricted by the electron density in the beam, ab.

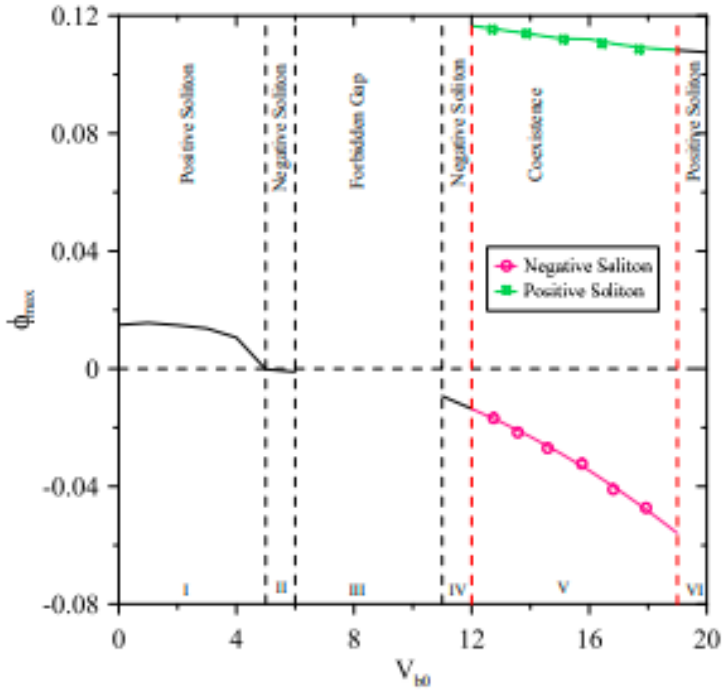

Figure 2. Existence domains of fast ion acoustic solitons as a function of normalized beam velocity Vb0 for given plasma parameters

The change of the critical Mach number, M0, as well as the maximum Mach number, Mmax, and the highest value of the potential, φmax, for the electron-acoustic mode is depicted in Figure 3. The normalized parameters for this mode are as follows: ni0 = 0.05, nb0 = 0.02, σp = 0.3, σi = 0.5, σb = 0.002, and κ = 6. It is just the negative potential soliton that is supported by the electron-acoustic mode.

In this case, we observe that the rise in Vb0 leads to an increase in both M0 and Mmax. The condition that the number density of beam electrons, denoted by nb, must be kept at a real value is the cause of the restriction placed on the largest amplitude that may be achieved.

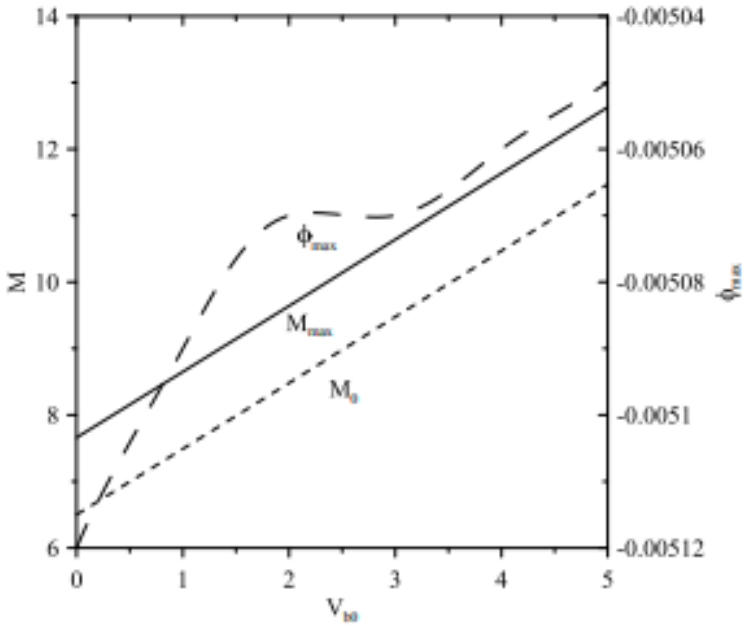

Figure 3: Variation of Mach numbers and maximum potential amplitude with normalized beam velocity Vb0 for electron acoustic mode

The left axis indicates Mach number and the right axis indicates potential amplitude

V. CONCLUSION

The existence and propagation properties of the electrostatic solitary waves have been logically investigated by using the Sagdeev pseudopotential method. The findings reveal the existence of the positive and negative potential solitons as well as the areas of restricted wave propagation or coexistence of various polarity structures. As it is seen, the parameters of plasma like the velocity of the electron beam and concentration and temperature of ions in a ratio are important in establishing the nature and stability of the solitary waves. The fact that slow and fast ion-acoustic modes are different only speaks to the complicated nature of nonlinear wave propagation. Also, only negative potential structures are observed to be supported by the electron-acoustic mode, due to the physical limitation of the plasma system.

REFERENCES: -

[1] Rasca, A., Fatemi, S., and Farrell, W., "Modeling the lunar wake response to a CME using a hybrid PIC model," *The Planetary Science Journal*, vol. 3, no. 1, pp. 1–8, 2022.

[2] Lakhina, G., Singh, S., Rubia, R., and Devanandhan, S., "Electrostatic solitary structures in space plasmas soliton perspective," *Plasma*, vol. 4, no. 4, pp. 681–731, 2021.

[3] Chu, F., Halekas, J., Cao, X., McFadden, J., Bonnell, J., and Glassmeier, K.-H., "Electrostatic waves and electron heating observed over lunar crustal magnetic anomalies," *Journal of Geophysical Research Space Physics*, vol. 126, no. 4, pp. 1–11, 2021.

[4] Sreeraj, T., Singh, S., and Lakhina, G., "Linear analysis of electrostatic waves in the lunar wake plasma," *Physica Scripta*, vol. 95, no. 5, pp. 1–15, 2020.

[5] Rubia, R., Singh, S., and Lakhina, G., "Occurrence of electrostatic solitary waves in the lunar wake," *Journal of Geophysical Research Space Physics*, vol. 122, no. 3, pp. 1–15, 2017.

[6] Haakonsen, C., Hutchinson, I., and Zhou, C., "Kinetic electron and ion instability of the lunar wake simulated at physical mass ratio," *Physics of Plasmas*, vol. 22, no. 3, pp. 1–9, 2015.

[7] Morozova, T., Kopnin, S., and Popel, S., "Wave processes in dusty plasma near the Moon's surface," *Plasma Physics Reports*, vol. 41, no. 10, pp. 799–807, 2015.

[8] Pickett, J., Kurth, W., Gurnett, D., Huff, R., Faden, J., Averkamp, T., Pisa, D., and Jones, G., "Electrostatic solitary waves observed at Saturn by Cassini inside 10 RS and near Enceladus," *Journal of Geophysical Research Space Physics*, vol. 120, no. 2, pp. 1–15, 2015.

[9] Varghese, S., Singh, K., and Kourakis, I., "On the morphology of electrostatic solitary waves in the Earth's aurora," *Scientific Reports*, vol. 12, no. 5, pp. 1–16, 2022.

[10] Pu, Z. Y., Shi, Q. Q., and Liu, W. L., "Three dimensional lunar wake reconstructed from ARTEMIS data," *Journal of Geophysical Research*, vol. 119, no. 2, pp. 5220–5243, 2014.

[11] Zhang, H., et al., "Outward expansion of the lunar wake ARTEMIS observations," *Geophysical Research Letters*, vol. 39, no. 2, L18104, 2012.

[12] Hashimoto, K., Hashitani, M., Kasahara, Y., Omura, Y., Nishino, M., Saito, Y., Yokota, S., Ono, T., Tsunakawa, H., Shibuya, H., Matsushima, M., Shimizu, H., and Takahashi, F., "Electrostatic solitary waves associated with magnetic anomalies and wake boundary of the Moon observed by KAGUYA," *Geophysical Research Letters*, vol. 37, no. 2, pp. 1–5, 2010.

[13] Kasahara, Y., Goto, Y., Hashimoto, K., Imachi, T., Kumamoto, A., Ono, T., and Matsumoto, H., "Plasma wave observation using waveform capture in the lunar radar sounder on board the SELENE spacecraft," *Earth Planets and Space*, vol. 60, no. 2, pp. 341–351, 2008.

[14] Farrell, W. M., Kaiser, M. L., and Steinberg, J. T., "Electrostatic instability in the central lunar wake a process for replenishing the plasma void," *Geophysical Research Letters*, vol. 24, pp. 1135–1138, 1997.

[15] Davidson, R. C., Krall, N. A., Papadopoulos, K., and Shanny, R., "Electron heating by electron ion beam instabilities," *Physical Review Letters*, vol. 24, no. 11, pp. 579–582, 1970.